Kumar and Murthy *Bioresour. Bioprocess.* (2017) 4:54
https://doi.org/10.1186/s40643-017-0184-2

Bioresources and Bioprocessing

RESEARCH

Open Access

Development and validation of a stochastic molecular model of cellulose hydrolysis by action of multiple cellulase enzymes

Deepak Kumar[1,2] and Ganti S. Murthy[1*]

Abstract

Background: Cellulose is hydrolyzed to sugar monomers by the synergistic action of multiple cellulase enzymes: endo-β-1,4-glucanase, exo-β-1,4 cellobiohydrolase, and β-glucosidase. Realistic modeling of this process for various substrates, enzyme combinations, and operating conditions poses severe challenges. A mechanistic hydrolysis model was developed using stochastic molecular modeling approach. Cellulose structure was modeled as a cluster of microfibrils, where each microfibril consisted of several elementary fibrils, and each elementary fibril was represented as three-dimensional matrices of glucose molecules. Using this in-silico model of cellulose substrate, multiple enzyme actions represented by discrete hydrolysis events were modeled using Monte Carlo simulation technique. In this work, the previous model was modified, mainly to incorporate simultaneous action enzymes from multiple classes at any instant of time to account for the enzyme crowding effect, a critical phenomenon during hydrolysis process. Some other modifications were made to capture more realistic expected interactions during hydrolysis. The results were validated with experimental data of pure cellulose (Avicel, filter paper, and cotton) hydrolysis using purified enzymes from *Trichoderma reesei* for various hydrolysis conditions.

Results: Hydrolysis results predicted by model simulations showed a good fit with the experimental data under all hydrolysis conditions. Current model resulted in more accurate predictions of sugar concentrations compared to previous version of the model. Model results also successfully simulated experimentally observed trends, such as product inhibition, low cellobiohydrolase activity on high DP substrates, low endoglucanases activity on a crystalline substrate, and inverse relationship between the degree of synergism and substrate degree of polymerization emerged naturally from the model.

Conclusions: Model simulations were in qualitative and quantitative agreement with experimental data from hydrolysis of various pure cellulose substrates by action of individual as well as multiple cellulases.

Keywords: Hydrolysis, Cellulase, Bioethanol, Modeling, Cellulase purification, Synergism

Background

During bioethanol production from lignocellulosic biomass, cellulose hydrolysis can be achieved using chemicals or biological catalysts (enzymes). Although acid hydrolysis is a relatively fast process, it suffers from some major limitations such as high operational cost, by-product formation, corrosion of equipment, neutralization requirement, high disposal cost (Bansal et al. 2009; Wang et al. 2012). Therefore, enzymatic hydrolysis is considered more feasible option during bioethanol production and has been the focus of research in last several decades. However, due to extensive hydrogen bonding, cellulose chains form a recalcitrant crystalline structure, which is difficult to degrade and require a much higher amount of

*Correspondence: Ganti.Murthy@oregonstate.edu
[1] Biological and Ecological Engineering, Oregon State University, Corvallis, OR, USA
Full list of author information is available at the end of the article

enzymes (40–100 times) for hydrolysis compared to that of starch (Merino and Cherry 2007; Wang et al. 2012).

Cellulose is hydrolyzed to glucose by synergetic action of multiple cellulase enzymes, such as endoglucanases (EG) (EC3.2.1.4), exoglucanases [also known as cellobiohydrolases (CBH)] (EC3.2.1.91) and β-glucosidase (BG) (EC3.2.1.21) (Bansal et al. 2009; Kadam et al. 2004; Zhang and Lynd 2004). Although all these enzymes have a different mode of action, they act in highly cooperative ("synergism") action for efficient degradation cellulose. Exoglucanases adsorb only from the chain ends (CBH I from reducing end and CBH II from the non-reducing end) and act in a processive manner to produce mainly cellobiose units. Processive enzymes remain bound to the glucose chain after cleaving a cellobiose molecule and will continue to cleave cellobiose units until a minimum chain length is reached. On the other side, endoglucanases are non-processive enzymes that act randomly on the surface glucose chains, hydrolyze one/few accessible internal bonds in the glucose chains and produce new chain ends. β-glucosidases hydrolyze the cellobiose and short soluble oligomers to glucose and complete the hydrolysis process (Fig. 1).

Due to high cost of cellulase enzymes (up to 30% of ethanol cost) and low sugar yields, the hydrolysis process is one of the major obstacles in the commercialization of cellulosic ethanol production (Bansal et al. 2009; Kadam et al. 2004; Kumar and Murthy 2011). There is potential for cost reduction by improving the understanding of the process, by testing a wide array of enzymes and various substrates under different conditions to determine optimum hydrolysis conditions. Designing highly efficient cellulase mixtures ("optimized enzyme cocktails") that can yield high hydrolysis rate at minimal enzyme dosage, is one such approach. Cellulase extracted from various microorganisms contain different amount of each enzyme and many commercial preparations consist of mixes from a different organism. For example, cellulase from *Trichoderma reesei* contains low fractions of β-glucosidase enzyme and this enzyme is added to the cellulase preparation to increase hydrolysis rates. It has been reported that synthetic enzyme mixture (designer combinations) of cellulase enzymes can give relatively higher hydrolysis yields (Ballesteros 2010; Banerjee et al. 2010a, b; Besselink et al. 2008). Currently, the only reliable method for designing optimal cellulase mixtures involves extensive experimentation using statistically designed combinations of various enzyme levels (Baker et al. 1998; Banerjee et al. 2010a, b; Berlin et al. 2007; Gao et al. 2010). Since conducting such large number of hydrolysis experiments is expensive, time-consuming and labor intensive, a comprehensive hydrolysis model that can that can capture process dynamics and predict hydrolysis profile under various scenarios could be an alternate feasible approach. However, due to multiple variables such as use of several enzymes acting synergistically, complex cellulose structure, and dynamic enzyme–substrate interactions make it difficult to develop mathematical models that can predict accurate hydrolysis profile under different operating conditions. Using a novel stochastic molecular modeling approach, in which each hydrolysis event is translated into a discrete event, we

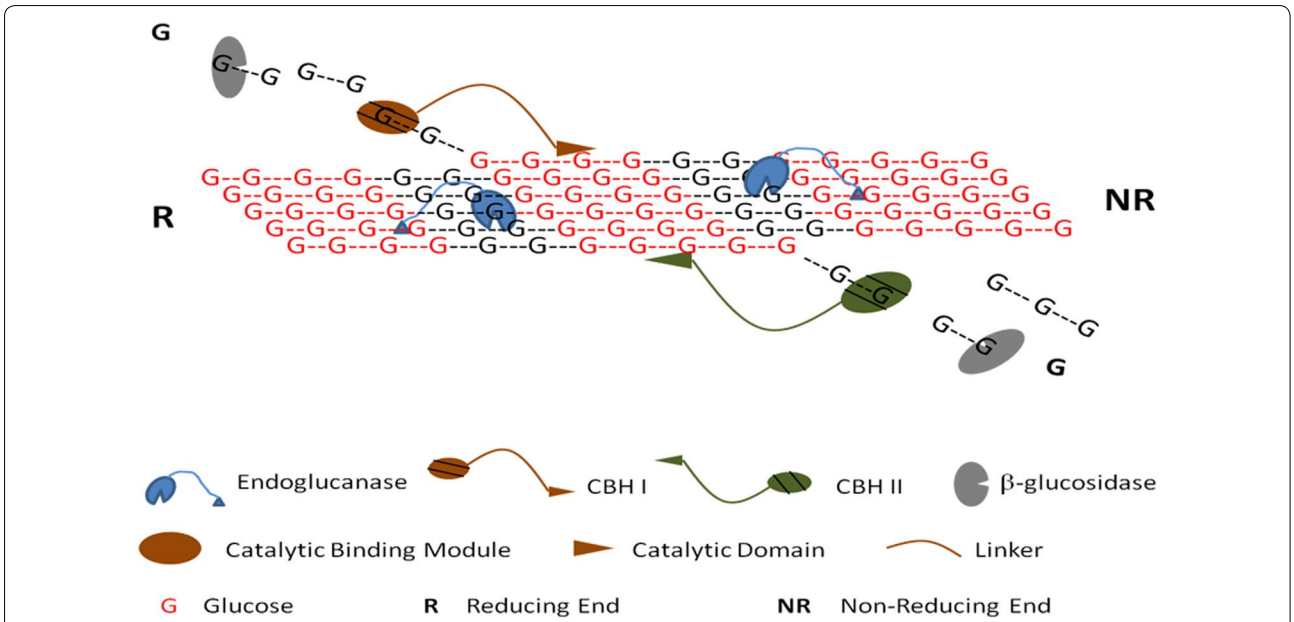

Fig. 1 Hydrolysis of cellulose by action of various cellulase enzymes. Red color represents crystalline region and black color are in amorphous region (Adapted from Kumar and Murthy 2013)

developed a first three-dimensional mechanistic cellulose hydrolysis model. The model captured the structural properties of cellulose, enzyme properties, the effect of reaction conditions, and most importantly dynamic changes in these properties (Kumar and Murthy 2013). Other than accurate predictions of hydrolysis profile, this modeling approach incorporates detailed structural features of cellulose and provides unique advantages compared to mathematical models, such as tracking of multiple oligomers as well as chain distribution, tracking of morphological changes in cellulose, elimination of the need for parameter changes with a change in experimental data set. Please refer to our earlier paper (Kumar and Murthy 2013) for more detailed comparison of this modeling approach and comparisons to other modeling approaches.

Although the previous model incorporated significant cellulose structural details and complex enzyme–substrate interactions, it did not include the simultaneous action of multiple classes of enzymes at any instant of time. During each iteration, only one class of enzymes (e.g., EG, CBH I or CBH II) was acting, which ignores the enzyme crowding/jamming effect, a critical phenomenon at high enzyme concentrations (Hall et al. 2010; Igarashi et al. 2011). This work presents the updated model with incorporation of enzyme jamming phenomenon by modeling simultaneous action of multiple enzymes, and also including other practical considerations, such as oligomer solubility and glucose production by cellobiohydrolase enzymes. Our earlier model was validated with very limited experimental data from the literature. In this work, the model simulations were validated with comprehensive experimental data sets obtained from hydrolysis of pure cellulose (Avicel, filter paper, and cotton) using purified *T. reesei* enzymes. Experiments were performed with purified CBH I and CBH II under various hydrolysis conditions, to cover the effect of enzyme loadings, substrate properties, and product inhibition.

Methods

Materials

Celluclast, a commercial cellulase from *T. reesei* (Lot # CCN03141), was donated by Novozymes (Novo, Bagsvaerd, Denmark). P-Aminophenyl β-D-cellobioside (sc-222106, Lot #K213), used as an affinity ligand for cellobiohydrolase, was purchased from Santa Cruz Biotechnology Inc. (Santa Cruz, CA, USA). All other chemicals required for protein purification and hydrolysis experiments were purchased from Sigma-Aldrich (Milwaukee, WI). Whatman No. 1 filter paper (Whatman, Inc., Florham Park, NJ) and cotton balls (Kroger Co., Cincinnati, Ohio) were used as the pure cellulose samples for the hydrolysis experiments. The commercial β-glucosidase (Novozyme 188) from *Aspergillus niger* was purchased from Sigma-Aldrich (Milwaukee, WI).

Model development

Stochastic hydrolysis model

Development of this comprehensive model consisting cellulose structural details and complex enzyme–substrate interactions consisted of in silico representative cellulose model, enzyme characterization, and developing algorithms for modeling the enzyme actions. In this model, cellulose was modeled based on the structure of cellulose Iβ, the most abundant cellulose form in higher plants. The structure was modeled as a group of microfibrils (MF) (2–20 nm diameter), and each microfibril contains multiple elementary fibrils (EF), the basic building block of cellulose with about 3.5 nm diameter and containing 36 glucose chains (Chinga-Carrasco 2011; Fan and Lee 1983; Lynd et al. 2002). The number of EF in an MF, glucose molecules in one chain of glucose (i.e., degree of polymerization, DP), was assumed to be constant during each simulation. These parameters were dynamically determined at the beginning of the cellulose structure simulation, based on the type of cellulose simulated. The degree of crystallinity in cellulose (50–90%) is a critical factor affecting the cellulose hydrolysis, as amorphous regions are believed to be relatively more susceptible to enzyme action and determine initial hydrolysis rates. To capture this important property in this model, glucose chain in each EF were assumed to pass through multiple crystalline regions (200 glucose molecules long regions) separated by amorphous regions. The concept of modeled cellulose structure and its resemblance with actual cellulose structure is illustrated in Fig. 2.

Each glucose molecule in the modeled microfibril was given a unique serial number as its identity, and a big data set containing other parameters (e.g., reducing/non-reducing end, EF surface, MF surface, crystalline or amorphous, soluble, non-soluble, distance from chain end, etc.) that describe structural properties of that bond. During developing algorithms for cellulase actions, enzyme accessibility was determined based on these parameters (data set with each glucose molecule) and action pattern of enzymes. For additional details of cellulose model please refer to earlier publications (Kumar 2014; Kumar and Murthy 2013).

Cellulase enzymes vary in mode of actions, and for this model, the enzymes were classified into eight classes depending upon their structure and mode of action (e.g., non-processive endocellulase with cellulose binding molecule (CBM), processive CBH I with CBM, processive CBH II with CBM, etc.). Please refer to our earlier paper (Kumar and Murthy 2013) for more details on enzyme classifications, their characteristics, and mode of actions. Cellulose hydrolysis is dependent on biomass-dependent extrinsic factors (crystallinity, accessibility, and DP) and enzyme action is dependent on intrinsic factors (enzyme

activity, stability with pH and temperature, etc.). The extrinsic factors were modeled in the simulated cellulose structure described above. Enzyme activity (depends on enzyme origin and level of purification) and enzyme loading (amount of enzyme/g substrate; based on experimental conditions) information was transformed into theoretical maximum turnover number (maximum possible number of bonds hydrolyzed per unit time for each enzyme) ($N_{\text{hi\_max}}$) (Eq. 1) for each class of enzyme.

$$N_{\text{hi\_max}} = E_i * U_i * 6.023 * 10^{17} * \frac{G_{\text{Sim}}}{6.023 * 10^{23}} * 162 * S_i, \quad (1)$$

where 'E_i' is amount of 'ith' enzyme used (mg cellulose); 'U_i' is activity of 'ith' enzyme (IU/mg enzyme); 'G_{sim}' is the number of glucose molecules simulated in the model; "162" is the average molecular weight of anhydrous glucose; 'S_i' is stability of 'ith' enzyme under experimental conditions (temperature and pH). Value of "S_i" could be calculated for any enzyme using empirical equations developed, such as Arrhenius rate relationship for temperature. Value of 'S_i' is a real number between 0 and 1.

These numbers were further transformed to numbers of hydrolyzed bonds per microfibril based on the total number of microfibrils simulated and mode of action of enzymes. For example, for endoglucanase enzymes, these numbers were proportional to relative glucose molecules on the surface of microfibril. On the other hand, for CBH I and CBH II, these numbers were proportional to a relative number of chain ends available in one microfibril. Please refer to Kumar (2014) for more details.

The hydrolysis process was modeled using Monte Carlo simulation technique, which has been used successfully earlier for modeling the starch hydrolysis (Marchal et al. 2001, 2003; Murthy et al. 2011; Wojciechowski et al. 2001). The overall schematic for simulating the enzymatic hydrolysis for each enzyme is shown in Fig. 3 and detailed description is provided in Kumar and Murthy (2013). All the required substrate–enzyme interactions, such as binding of CBH only on chain ends, the higher binding probability of binding EG on MF surface than at EF surface, were incorporated into the model using algorithms. It was also made sure that sufficient glucose molecules (based on the size of enzyme) are available to allow binding.

Only one class of enzymes was modeled working at a time, so the model did not account for the enzyme crowding effect (locations occupied by other class of enzymes at the same time). These effects were incorporated in the modified model discussed in next section. Other than cellulose structural restrictions, some probabilities were

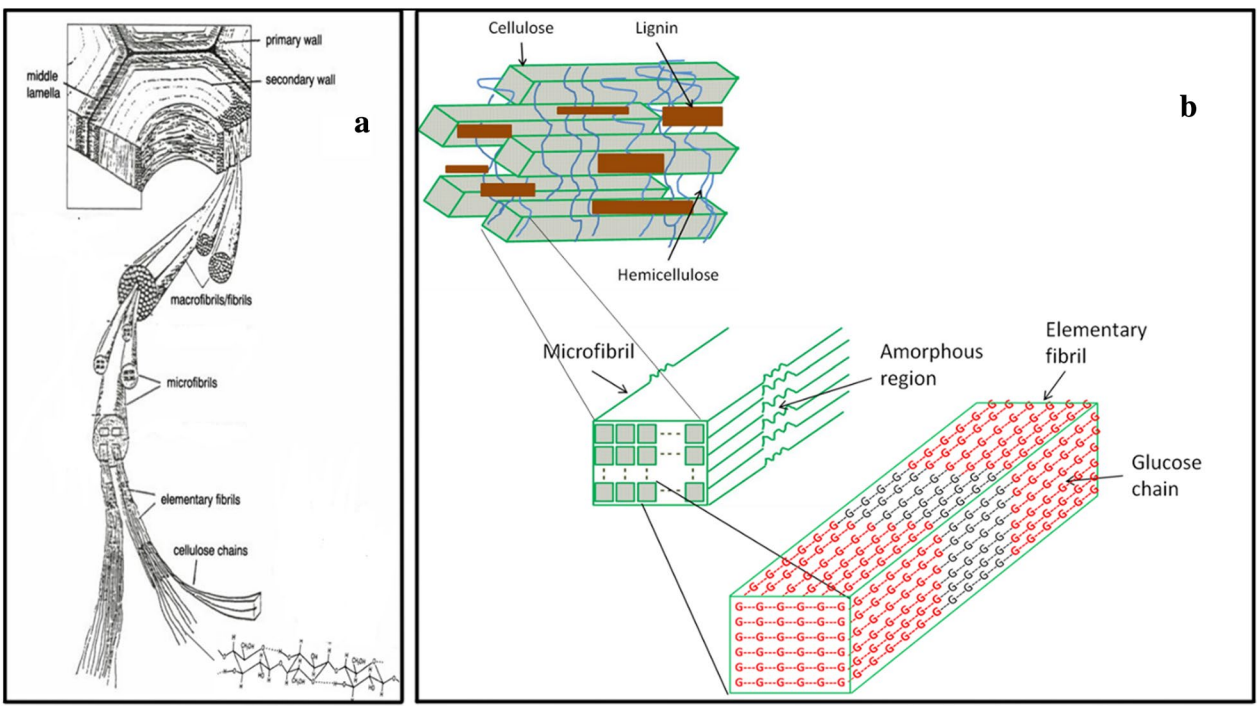

Fig. 2 Structure of cellulose: **a** actual cellulose structure; **b** structure of cellulose simulated in model. Glucose molecules in red color represent crystalline region and glucose molecules in black color are in amorphous region. (Adapted from Kumar 2014)

defined corresponding to enzyme action. For example, the probability of hydrolysis of a β-1,4 bond hydrolysis located in amorphous regions was more than that of in crystalline region by an endoglucanase enzyme. Choice was made by generating a random number at each decision point and comparing it with the defined probability. The hydrolysis event would happen only in the case when the random number was greater than the probability of hydrolysis. Number of iterations were restricted using a counter (Fig. 3). If all conditions for hydrolysis were met for that bond, it was converted to broken bond and the counter was incremented. Similarly, the counter was given an increment corresponding to unsuccessful events also (in case binding or hydrolysis does not occur). After each broken bond, it was made sure to change properties of other glucose molecules in that chain (e.g., chain length, distance from chain end, solubility, etc.). If a glucose chain becomes soluble, part of the chain just beneath the soluble chain is exposed and becomes accessible to enzymes. The concept is described in detail elsewhere (Kumar 2014).

Modifications in the model

The model described in above section was the first report of a comprehensive stochastic model for cellulose hydrolysis that successfully captured the cellulose structural features (three dimensional), enzyme characteristics, and dynamic enzyme–substrate interactions. In this work, the model was further modified to capture more realistic expected interactions during hydrolysis by incorporating the (1) simultaneous action of enzymes from multiple classes at any instant of time to account for the enzyme crowding; (2) partial solubility of cello-oligomers with DP 6–13, and (3) production of glucose by exocellulase. In the previous version of the model, the model was simulated based on the iterative concept only; however, in real conditions multiple enzyme molecules act simultaneously and block the hydrolysis sites for each other (Igarashi et al. 2011). Enzyme crowding and simultaneous action of enzymes were incorporated in the current model by calculating the number of enzyme molecules based on the enzyme loading, their molecular weight, and number of glucose molecules simulated. The iterations are performed for every minute of hydrolysis and properties of substrate are changed after that at the end of the 1-min time step. For processive enzymes, once an enzyme molecule bound to chain end, it remains bound at the end of 1-min time step and continues further down the chain until it reaches the end of the chain or desorbs from the molecule as per its probability. Exocellulase enzyme binds to multiple cellulase chains (three chains in the model) (Asztalos et al. 2012; Levine et al. 2010), so it is essential that all three chains must be accessible to the enzyme (on surface and not blocked by other enzyme) for binding of the enzyme. In the previous version of model, it was assumed that glucose molecules equal to size of CBM only are required on surface and unblocked for binding, however in the current model whole length of enzyme was considered (except linker, because it is flexible and is compressed during movement) (Wang et al. 2012). The detailed schematics explaining algorithms developed to model CBH I and EG actions have been provided in the in Additional files 1 and 2, respectively. Cellodextrins with DP < 6 are considered to be completely soluble, DP 6–13 partially soluble and above 13 are insoluble in water (Lynd et al. 2002; Zhang and Lynd 2004). In the previous version of the model, all oligomers with DP > 6 were considered insoluble. While the CBM of the enzymes cannot bind to these chains due to its large size, the catalytic domains of the enzymes will still act on the oligomers in solution. In the absence of reliable literature data, the soluble fraction of the oligomers was set as a function of DP in the range of DP 7–13. The oligomers with DP 7–9, 10–11, and 12–13 were assumed 75, 50, and 25% soluble, respectively. Oligomers with DP < 6 were assigned a 100% solubility, and while oligomers with DP more than 13 were set to 0% solubility. In the previous model, the CBH action could only produce cellobiose during cellulose hydrolysis. However, glucose formation during cellulose hydrolysis by CBH action has been observed by some researchers (Eriksson et al. 2002; Medve et al. 1998), and was also observed in our experiments (discussed later in the "Results and discussion" section). Therefore, the model was modified to include glucose formation in addition to the cellobiose. A probability of glucose formation was included in the model, and glucose/cellobiose formation was decided by generating a random number and comparing with that probability. The probabilities and increments associated with productive various events (productive binding, no binding, non-productive binding, etc.) are listed in Additional file 3: Table S1.

Enzyme crowding/jamming phenomenon might not be critical at low enzyme dosages and during action of individual enzymes. Also, the other details incorporated into this model might be ignored if the final goal of the model is to simulate the sugar concentration only during the hydrolysis process. However, to simulate and optimize the composition/cocktail of enzymes, it is necessary to simulate the effects of each enzyme class carefully.

Model implementation and simulations

The algorithms of the hydrolysis model were written in C++ language. Random number generators were used in simulation of cellulose structure and hydrolysis process (Matsumoto and Nishimura 1998).

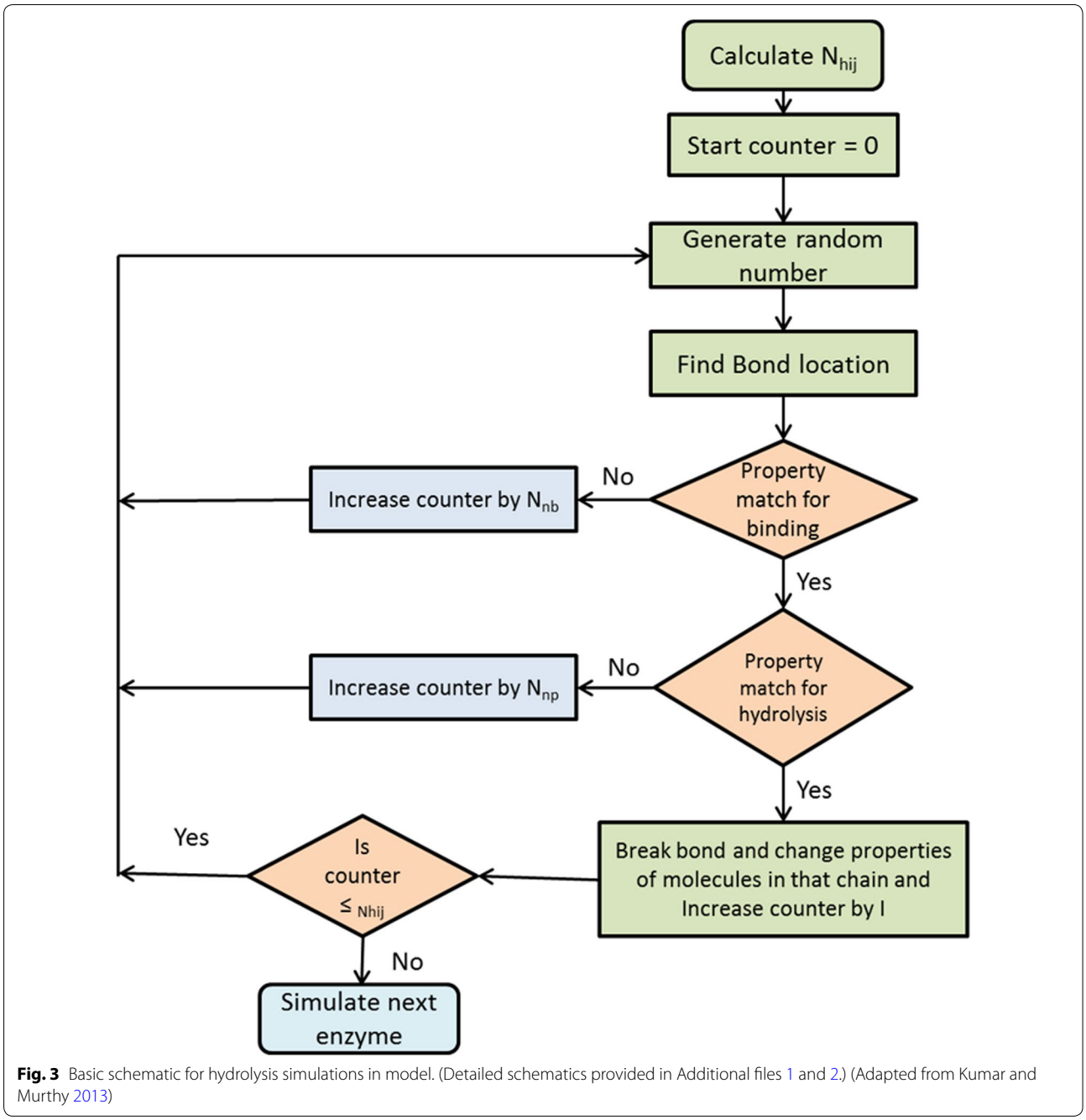

Fig. 3 Basic schematic for hydrolysis simulations in model. (Detailed schematics provided in Additional files 1 and 2.) (Adapted from Kumar and Murthy 2013)

The cellulose structure was simulated for three model cellulose substrates Avicel, filter paper and cotton, to cover the range of substrates with different structural properties (DP and degree of crystallinity). Avicel is low-DP cellulose, with DP only about 300 and crystallinity index 0.5–0.6; whereas, cotton has relatively very high DP (about 2000–2500) and crystallinity index of 0.85–0.95 (Zhang and Lynd 2004). Hydrolysis simulations were performed based on the experimental conditions: weight of solution (scale of hydrolysis), solid loading, cellulose content, total enzyme loading (mg protein/g cellulose), ratio of enzymes present (EG:CBH I:CBH II:BG), temperature, pH and hydrolysis duration. Enzyme activities can be determined from supplier, literature, or can be determined using standard protocols (Ghose 1987). Unless determined in the lab, specific activities of enzymes from *T. reesei* were assumed as 0.4, 0.08, and 0.16 IU/mg of EG I, CBH I and CBH II, respectively (Zhang and Lynd 2006) for model simulations. The output from model included several data files containing glucose concentrations,

oligosaccharide concentrations, chain distribution profile (number of chains of various lengths), crystallinity index profile (ratio of crystallinity at various time intervals), solubility profile and data sheets for each microfibril (illustrating major properties associated with glucose molecules) at various times during hydrolysis.

Model validation

The data from model simulations were compared with various sets of experimental results from cellulose hydrolysis in our lab and from literature (Bezerra and Dias 2004; Bezerra et al. 2011) to validate the model under various hydrolysis conditions.

Validation with experimental data

The model was validated with the results obtained from hydrolysis of pure cellulosic substrates (filter paper and cotton) using purified CBH I and CBH II. The cellulases CBH I and CBH II were purified from Celluclast (Novozymes, Denmark) using a series of chromatography steps in BioLogic LP system (Bio-Rad Laboratories, Hercules, CA, USA). The purification experiments were performed at room temperature and the collected enzymes were transferred and stored in the refrigerator at 4 °C.

Enzyme purification

The flow diagram of steps followed in the CBH I and CBH II purification is shown in Fig. 4. In the first step of purification, the Celluclast enzyme mixture was desalted using Sephadex G-25 Fine (dimensions: 2.5 cm × 10 cm) gel filtration column. The protein was rebuffered in 50 mM Tris–HCl buffer (pH 7.0) at 5 mL/min. The desalted protein was fractionated by anion-exchange chromatography using DEAE-Sepharose column (dimensions: 2.5 cm × 10 cm). The sample was loaded using 50 mM Tris–HCl buffer (pH 7.0) at 5 mL/min flow rate and was eluted stepwise: 1st elution at 35%, and 2nd elution at 100% of 0.2 M sodium chloride in 0.05 M Tris–HCl buffer (pH 7) (Jäger et al. 2010). The flow-through from DEAE column (rich in CBH II enzymes) was concentrated and rebuffered in 50 mM sodium acetate buffer (pH 5.0) using Pellicon XL 50 Ultrafiltration Cassette, with biomax 10 (Millipore, USA). The rebuffered protein was spiked with gluconolactone (final concentration of 1 mM) and loaded on the p-aminophenyl cellobioside (pAPC) affinity column (dimensions: 1.5 cm × 10 cm) with 0.1 M sodium acetate, containing 1 mM gluconolactone and 0.2 M glucose (pH 5.0) at flow rate of 1.5 mL/min (Jeoh et al. 2007; Sangseethong and Penner 1998). The function of gluconolactone in the buffer is to suppress β-glucosidase activity, which otherwise can cleave the ligand (Sangseethong and Penner 1998). The bound CBH II protein was eluted using the running buffer containing 0.01 M cellobiose [100 mM sodium acetate buffer containing 1 mM gluconolactone, 0.2 M glucose, and 0.1 M cellobiose (pH 5.0)]. The purified CBH II from affinity column was concentrated and loaded on the phenyl Sepharose column (dimensions: 1.0 cm × 10 cm) for hydrophobic interaction chromatography to separate core and intact proteins (Sangseethong and Penner 1998). The sample was loaded in high salt (0.35 M ammonium sulfate in 25 mM sodium acetate buffer, pH 5.0) and eluted with linear gradient from running buffer to elution buffer [25 mM acetate buffer containing 20% ethylene glycol (v/v), pH 5.0]. Hydrophobic interaction chromatography was performed on the second elution (CBH I rich) from the anion-exchange column, after concentrating and rebuffering with 25 mM sodium acetate buffer. The enzyme was loaded in very high salt (0.75 M ammonium sulfate in 25 mM sodium acetate buffer, pH 5.0) and eluted with linear gradient from running buffer to elution buffer [25 mM acetate buffer containing 5% ethylene glycol (v/v), pH 5.0]. The purified CBH II and CBH I fractions from hydrophobic interaction column were concentrated and rebuffered in 50 mM sodium acetate buffer, pH 5.0. Protein containing fractions were determined by measuring absorbance at 280 nm.

The fractions collected from the chromatographic purifications steps shown in Fig. 4 were analyzed by SDS-polyacrylamide gel electrophoresis to check for their purity. Based on the molecular weight comparison with marker, and literature data, the single bands in the numbered lanes 1 and 2 of Fig. 5 correspond to CBH II (MW 54 kDa) and CBH I (MW 61–64 kDa), respectively (Jäger et al. 2010; Medve et al. 1998; Sangseethong and Penner 1998). The activities of CBH I and CBH II on Avicel were determined as 0.478 and 0.379 IU/mg of protein, respectively.

During protein purification, the protein concentrations in the samples were determined based on Bradford assay using Quick Start™ Bradford Protein Assay Kit (Bio-Rad, USA) and bovine serum albumin (BSA) as standard. The activities of purified CBH I and CBH II were determined on Avicel in 50 mM sodium acetate buffer, pH 5.0. 1 mL of Avicel solution (10 g/L) with final enzyme concentration of 0.1 mg/mL was incubated (mixed end to end) at 45 °C in 2 mL Eppendorf centrifuge tubes for 2 h (Jäger et al. 2010). After 2 h of incubation, the samples were heated at 95 °C for 5 min to stop the hydrolysis. The samples were centrifuged at 15,000 rpm for 5 min to separate the supernatant. The reducing sugar concentration in the supernatant was determined using dinitrosalicylic acid (DNS) assay and using glucose as standard.

Enzymatic hydrolysis

The hydrolysis experiments were conducted at 25 g/L cellulose (filter paper and cotton balls) concentration

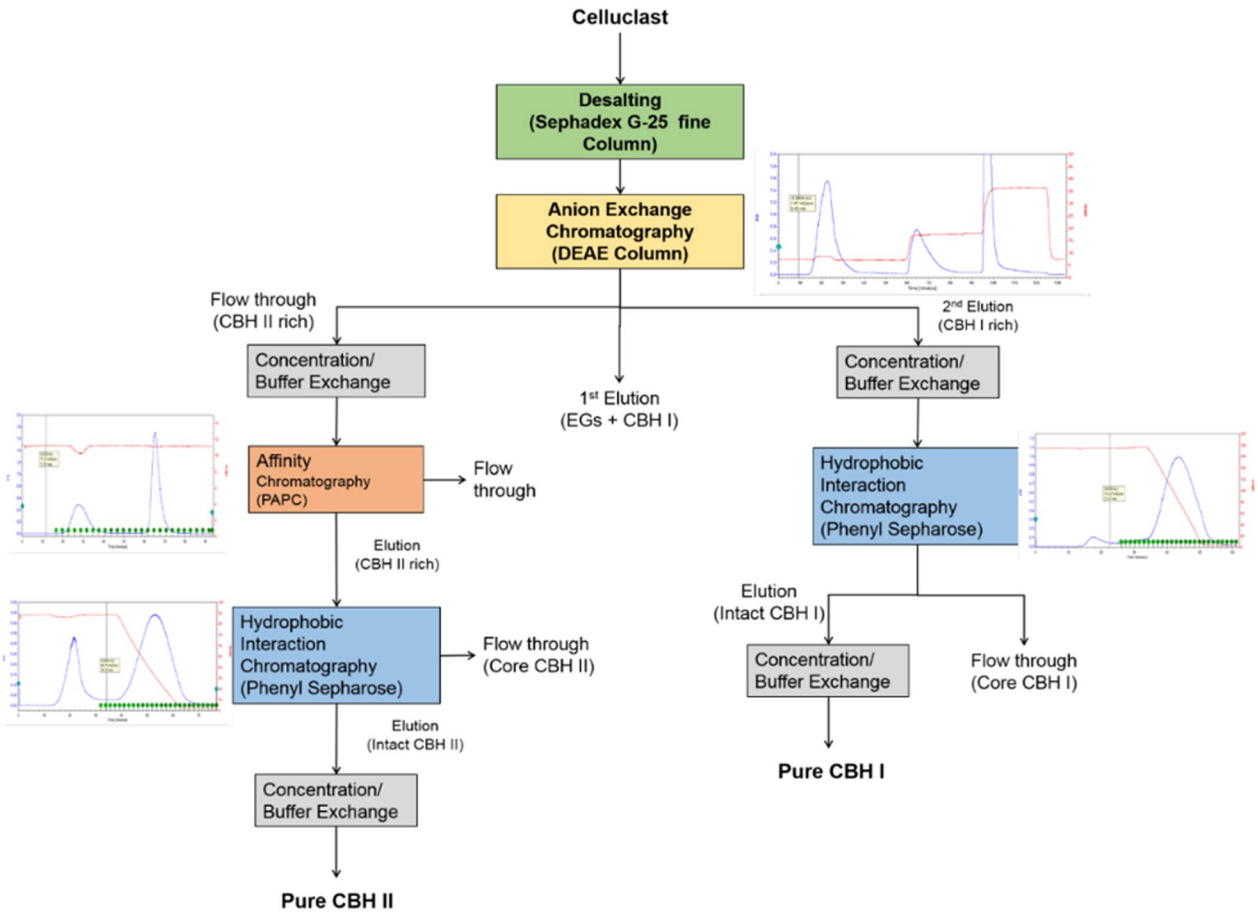

Fig. 4 Flow diagram of the chromatography steps used for purification of the CBH I and CBH II enzymes. Blue lines in the sub-plots refer to absorbance at 280 nm and red line refers to conductivity

and various enzyme loadings (5, 10, and 15 mg/g cellulose) in 50 mM sodium acetate, pH 5.0, 10 mL total volume in 25 mL Erlenmeyer flasks closed with rubber stopper. 100 µL of 2% sodium azide was added in each flask to avoid microbial contamination. The experiments were carried out in controlled environment incubator shaker set at 45 °C and 125 rpm. 200 µL of sample was withdrawn at 3, 6, 9, 12, 18, 24, 36, 48, and 72 h to determine sugar concentrations and the hydrolysis profile. The samples were heated at 95 °C for 5 min to stop the reaction and were prepared for high-performance liquid chromatography (HPLC) analysis. All experiments were performed in triplicate.

Results and discussion

Validation with literature data

Model simulations were performed for Avicel hydrolysis by CBH I using experimental conditions mentioned in Bezerra and Dias (2004). Figures 6 and 7 illustrate the comparison of model simulations and experimental data from hydrolysis of cellulose at 5 and 2.5% solid loadings, respectively. The data from simulation of previous version of model (Kumar and Murthy 2013) were also plotted in these figures to demonstrate the differences in hydrolysis profiles. Results from experimental data and model simulation data were in qualitative and quantitative agreement at both 25 and 50 g/L Avicel loadings. Coefficient of determination (R^2) was found 0.97 (at 5% Avicel loading) and 0.94 (at 2.5% Avicel loading) and was higher than that obtained from previous model results: 0.70 (at 5% Avicel loading) and 0.89 (at 2.5% Avicel loading). Coefficient of determination value was low for previous version of model because, at such high enzyme loadings, enzyme crowding effect become predominant, which was not captured in the previous version of model. Current model captures the crowding effect and therefore results in more accurate cellobiose concentrations. Quantitative match of model simulations with experimental data for various substrate–enzyme ratios also indicated that this model successfully captured the

cellobiose inhibition effect. Comparison of model simulations with additional experimental data from literature (lower enzyme loadings) is illustrated in Additional file 3: Figures S1a and S1b.

Validation with experimental data from current study

Hydrolysis of filter paper by CBH I and CBH II

The results from model simulations and actual experiments of hydrolysis of filter paper at various loadings of CBH I and CBH II are shown in Figs. 8, 9, 10 and 11, respectively.

In all of the cases, the model fitted filter paper hydrolysis data and predicted the sugar profiles and hydrolysis rates. It is very important to note that except enzyme activities (determined experimentally in this case), no other model parameter was changed during simulations under these hydrolysis conditions vs. earlier literature-based experimental conditions. Excellent fitting of model with data with studies from two different lab groups demonstrates the robustness and potential usability (scope of using for any hydrolysis conditions with parametrization issues) of this model. As expected, cellobiose, followed by glucose was the major product during hydrolysis by CBH I or CBH II. The model predictions were accurate in determining both cellobiose and glucose concentrations during hydrolysis. The previous version of model did not account for the glucose formation during cellulose hydrolysis by cellobiohydrolases, hence, did not fit with the experimental data (Additional file 3: Figure S2). Small amounts of cellotriose were also observed both in experimental data and model simulations (data not shown). The cellobiose production rate is high at the beginning of hydrolysis and decreases significantly due to cellobiose inhibition on the CBH I and II enzymes. The inhibition effect was captured by the model and was also further validated when the effect disappears on removal of cellobiose by converting it to glucose through β-glucosidase action (discussed later in the manuscript).

The R^2 values between experimental and model data for cellobiose production during filter paper hydrolysis by CBHI and CBH II were in the range of 0.65–0.90 and 0.77–0.81, respectively. It was observed from the results that increase in enzyme loading did not result in the significant increase in the final sugar yields. The enzymes used in the hydrolysis experiments had very high activity, and possibly increasing the enzyme loading resulted in the enzyme crowding effect due to limited availability of chain ends. It can be observed from the results, that the phenomenon was well captured by the model, as the simultaneous action of multiple enzyme, their blockage by each other was considered in the model.

Effect of beta-glucosidase addition (exo-BG synergism)

Cooperative action of different enzymes, known as synergism, is one of the most important phenomenon observed in cellulose degradation (Andersen et al. 2008; Bansal et al. 2009; Wang et al. 2012; Zhang and Lynd 2004). Synergism between CBH I and/or CBH II and β-glucosidase enzymes is very important for the conversion of cellulose (Zhang and Lynd 2004). This synergism

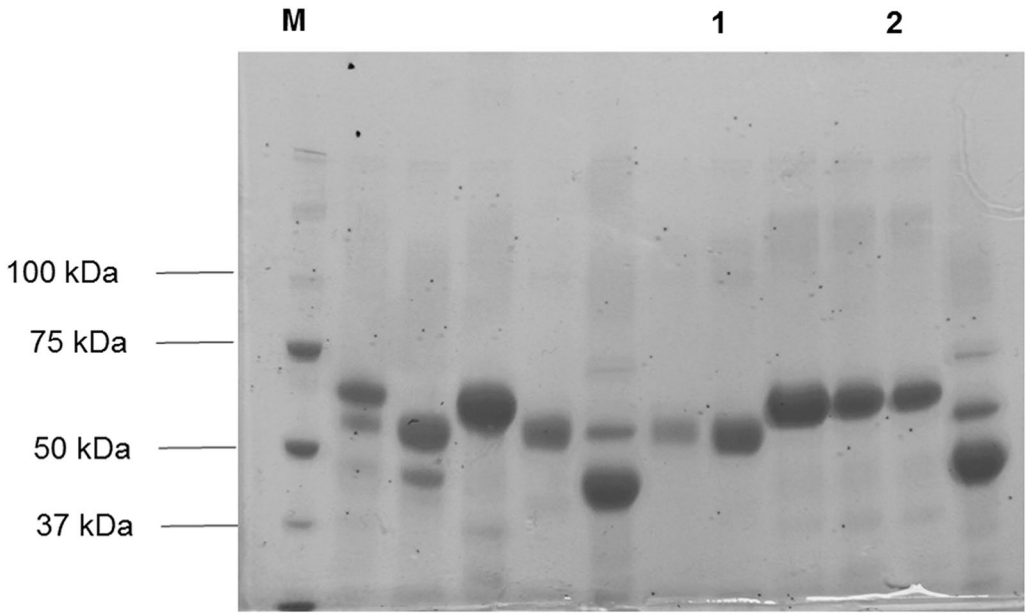

Fig. 5 SDS-polyacrylamide gel electrophoresis of the purified cellulase enzymes. *M* molecular mass marker, (1) CBH II (2) CBH I

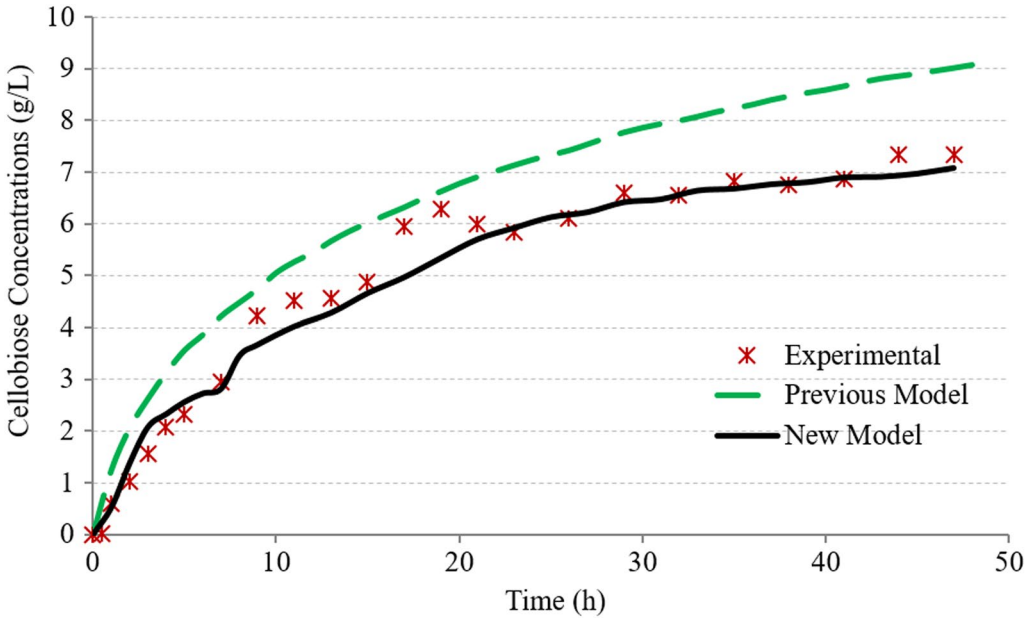

Fig. 6 Comparison of model simulations (current and previous version) and experimental data of cellobiose production during hydrolysis of Avicel (50 g/L) at 20 mg/g cellulose loading. The data points are from literature studies (Bezerra and Dias 2004; Bezerra et al. 2011), solid lines are from the new model predictions, and dotted lines are for predictions from previous version of model

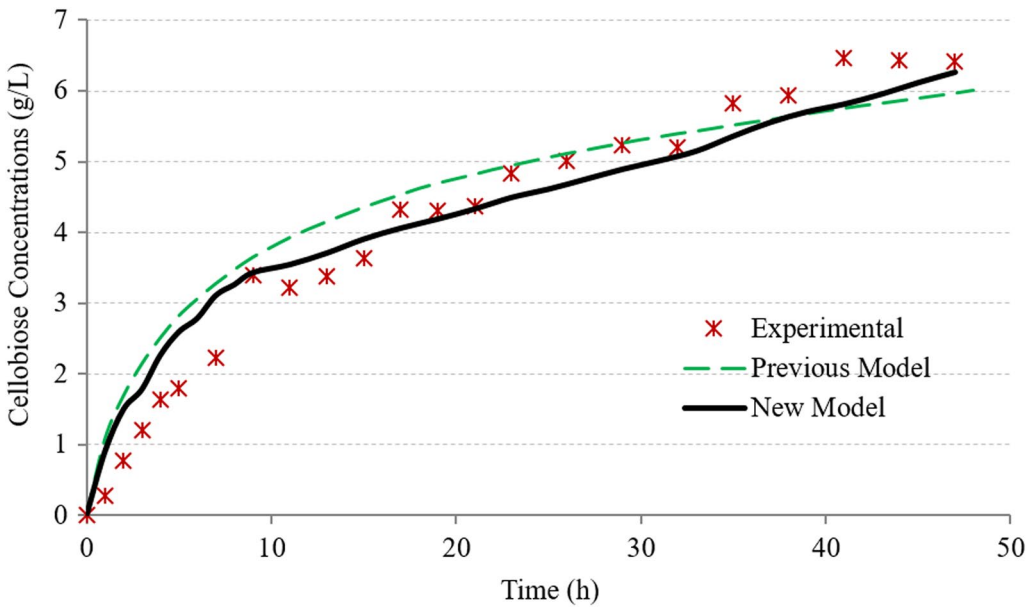

Fig. 7 Comparison of model simulations (current and previous version) and experimental data of cellobiose production during hydrolysis of Avicel (25 g/L) at 40 mg/g cellulose loading The data points are from literature studies (Bezerra and Dias 2004; Bezerra et al. 2011), solid lines are from the new model predictions, and dotted lines are for predictions from previous version of model

occurs mainly because of strong inhibition effect of cellobiose on the CBH performance. Primary product of CBH action on cellulose is cellobiose, a strong inhibitor to CBH activity (Andersen 2007; Ballesteros 2010; Fan et al. 1987; Mosier et al. 1999; Zhang and Lynd 2004). Cellobiose buildup is prevented by the action of β-glucosidase which further hydrolyzes cellobiose to glucose and results in CBH and β-glucosidase synergism. The synergistic

effect of β-glucosidase addition was observed during filter paper hydrolysis by CBH I and CBH II and is illustrated in Figs. 12 and 13, respectively.

Cellulose conversions after 72 h of hydrolysis were observed about 82.7 and 15.1% higher for CBH I (10 mg/g glucans) and CBH II (10 mg/g glucans), respectively, in presence of excess β-glucosidase than those in absence of β-glucosidase. To determine the model accuracy in predicting this trend, action of CBH I and CBH II was simulated in absence and presence of β-glucosidase. It can be observed from Figs. 11 and 12 that model simulations capture this synergism successfully both for CBH I and CBH II enzymes.

The synergism was lower for CBH II compared to CBH I, possibly due to relatively less inhibitory effect of cellobiose on CBH II. The observation of relatively lower cellobiose inhibition towards CBH II was also reported in a comprehensive study on cellobiose inhibition using ^{14}C-labeled cellulose substrates, conducted by Teugjas and Väljamäe (2013). In that study, it was reported that enzymes from glycoside hydrolase (GH) family 7 were most sensitive to cellobiose inhibition followed by family 6 CBHs and endoglucanases (EGs). The model simulations successfully followed the trend observed experimentally. Other than cellulose conversion, hydrolysis rate of filter paper by CBH I and CBH II with excess

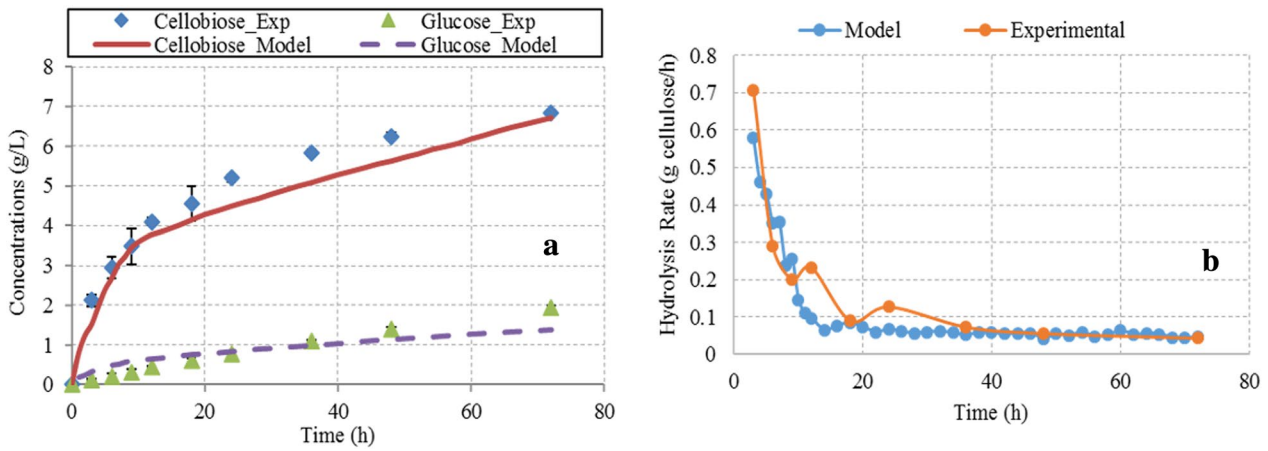

Fig. 8 Comparison of model simulations (solid lines) with experimental data during hydrolysis of filter paper (25 g/L) at CBH I loading of 10 mg/g cellulose: **a** sugar production, **b** rate of conversion of cellulose

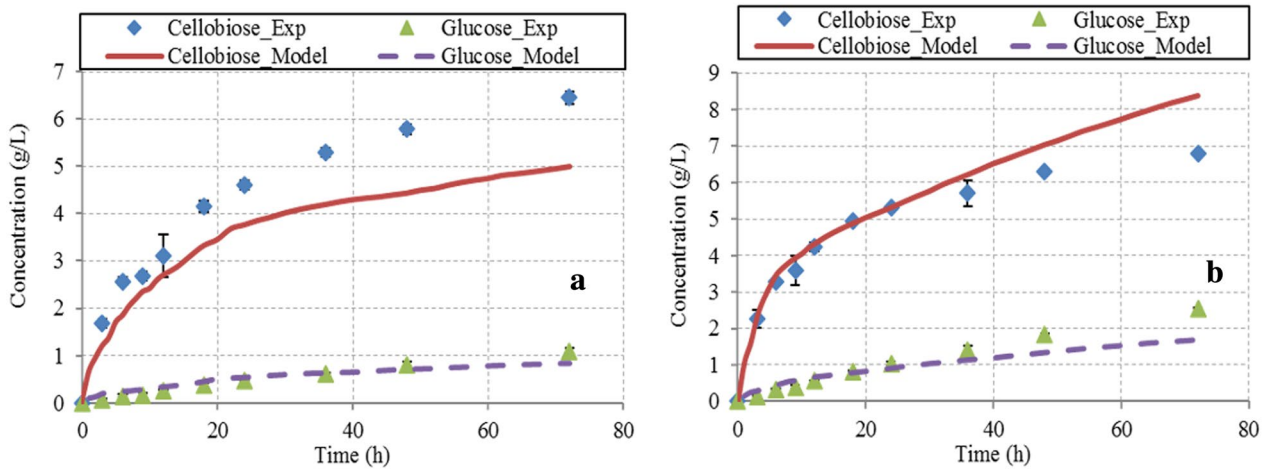

Fig. 9 Comparison of model simulations and experimental observations of sugar production during hydrolysis of filter paper (25 g/L) at **a** CBH I loading of 5 mg/g cellulose, **b** CBH I loading of 15 mg/g cellulose

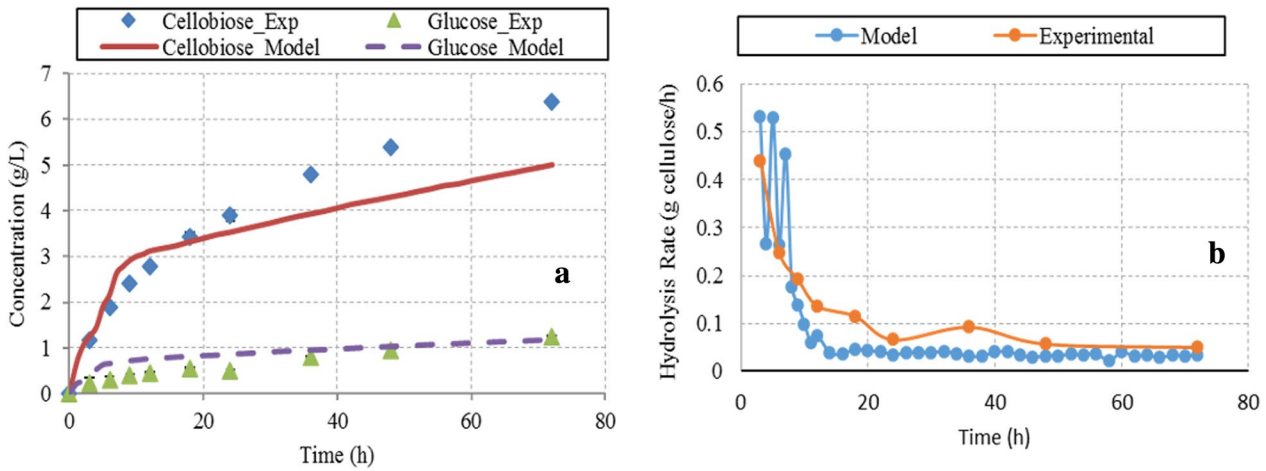

Fig. 10 Comparison of model simulations (solid lines) with experimental data during hydrolysis of filter paper (25 g/L) at CBH II loading of 10 mg/g cellulose: **a** sugar production, **b** rate of conversion of cellulose

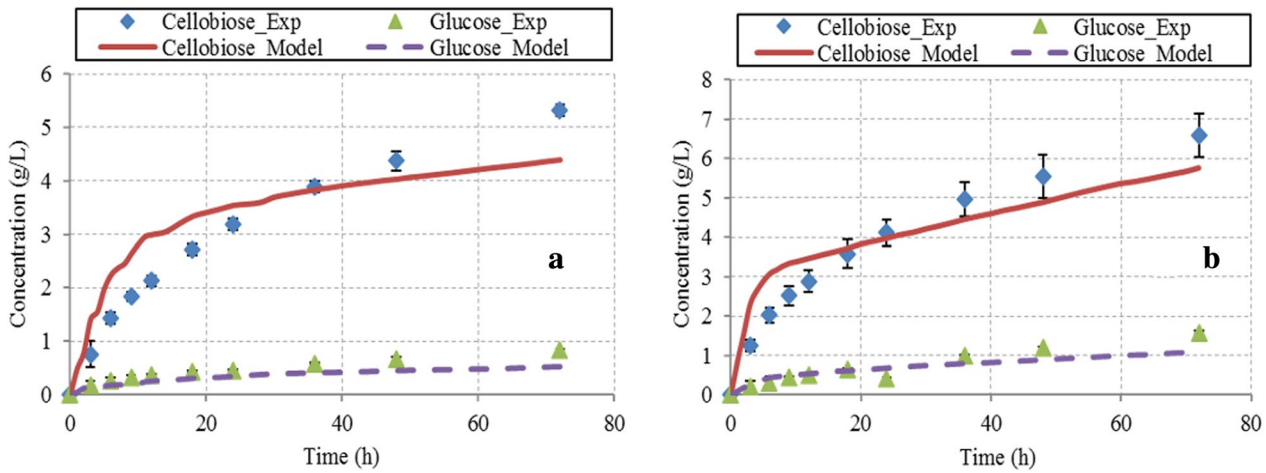

Fig. 11 Comparison of model simulations and experimental observations of sugar production during hydrolysis of filter paper (25 g/L) at **a** CBH II loading of 5 mg/g cellulose, **b** CBH II loading of 15 mg/g cellulose

of β-glucosidase was markedly higher than that of CBH enzymes acting alone (data not reported).

Effect of structural properties of cellulose

Cellulose hydrolysis is highly affected by the structural properties of cellulose. In case of cellobiohydrolases (CBH I and CBH II) action, where the enzymes act on chain ends only, fractions of reducing/non-reducing ends relative to total glucose molecules would be critical factor affecting hydrolysis. For example, the percentage of chain ends for filter paper with average chain DP of 700 is 0.13% compared to 0.05% for bacterial cellulose with average DP of 2000 and 0.033% for cotton with DP of 3000 (Zhang and Lynd 2004, 2006). Therefore, it would be expected that CBH I and CBH II would hydrolyze filter paper more efficiently compared to cotton or bacterial cellulose, as there are relatively many more reducing/non-reducing ends. The expected trends were observed in both experimental and model simulations of CBH I and CBH II action on filter paper and cotton (Fig. 14a, b).

The cellulose conversion after 72 h of cotton hydrolysis was observed 77.0 and 92.6% less than those of filter paper hydrolysis by action of CBH I and CBH II, respectively. The model had a good fit with experimental data for cotton hydrolysis in case of CBH I. For CBH II, although the absolute values of predicted cellulose conversion were

higher than the actual values, the expected trend was observed. So, the model simulations successfully captured the inverse relationship between substrate DP and hydrolysis of cellulose and predicted 73 and 81.1% reduction in cellulose conversion for cotton compared to filter paper for CBH I and CBH II, respectively. Similar results have been reported in literature from both experimental as well as modeling studies (Wood 1974; Zhang and Lynd 2006).

As endoglucanases act on the surface chains, their activity is not severely affected by fraction of chain ends; however, degree of crystallinity plays an important role in deciding their performance. Bonds in the amorphous region are more susceptible to hydrolysis compared to those in crystallinity regions because of higher accessibility of enzymes in amorphous regions (Chang and Holtzapple 2000). This behavior was also successfully captured by model simulations as cellulose conversion by action of endoglucanases on cotton (highly crystalline cellulose, CrI 0.85–0.90) was found 57.2% lower than that of filter paper (semi-crystalline cellulose, CrI 0.4–0.5) after 48 h of hydrolysis (Additional file 3: Figure S3).

Other model simulations

Enzymatic hydrolysis of cellulose by individual enzymes

As discussed in sections above, model was simulated for filter paper hydrolysis by action of individual cellulase enzymes. Hydrolysis rates during action of individual enzymes (EGI, CBH I and CBH II) on filter paper (25 g/L) are presented in Fig. 15. For all enzyme classes, there was significant drop in hydrolysis rates after few initial hours of hydrolysis and then the rate became nearly constant. This decrease in rate after few hours of initial hydrolysis is widely an observed phenomenon and is believed to occur due to morphological changes in the cellulose structure (e.g., decrease in glucose chains on the surface, increased percentage of crystallinity regions). These changes affect the enzyme–substrate interactions by limiting the accessibility of cellulase enzymes to glucose chains and results in rapid decline in hydrolysis rate (Zhang and Lynd 2004; Zhou et al. 2009). As observed in experimental results also, cellobiose is the major product formed during cellulose hydrolysis by CBH I and CBH II, which also acts as a strong inhibitor to these enzymes and negatively affects the hydrolysis rate.

After 48 h hydrolysis of filter paper by EG I, it was observed (from model simulations) that concentrations of oligomers with DP 2–4 and glucose were higher compared to cellopentaose and cellohexaose concentrations (Additional file 3: Figure S4). There was increase in concentrations of cellopentaose and cellohexaose during initial few hours (3–4 h), and after that their concentrations started decreasing. This trend was also expected because of change in availability of glucose molecules on surface. Surface glucose chains are easily accessible during initial phase of hydrolysis, where endoglucanases act randomly to producing short chains. As the hydrolysis progress, availability of these glucose chains decreases, and enzymes start acting on soluble sugars. Concentration of sugars with DP 2–4 did not decrease as EG I

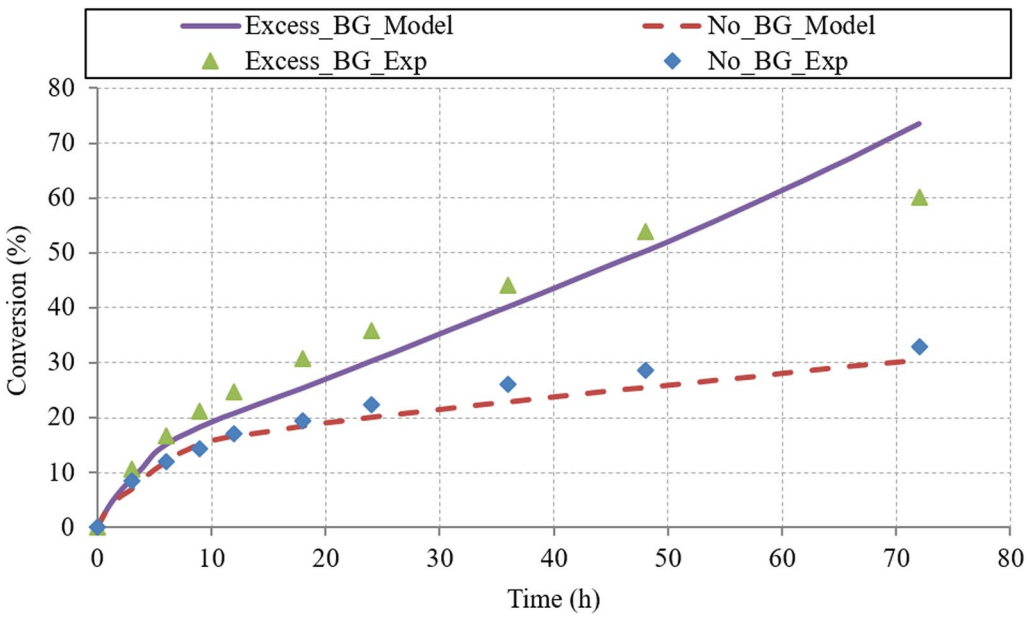

Fig. 12 Effect of β-glucosidase addition on cellulose hydrolysis by CBH I (25 g/L filter paper; CBH I: 10 mg/g cellulose)

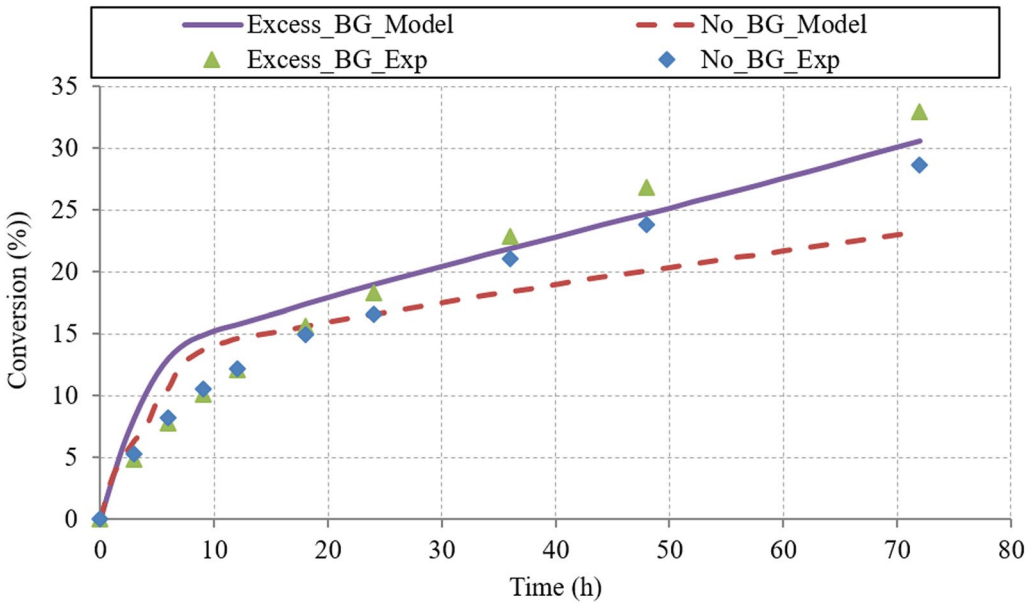

Fig. 13 Effect of β-glucosidase addition on cellulose hydrolysis by CBH II (25 g/L filter paper; CBH II: 10 mg/g cellulose)

was assumed to act only on oligomers with DP > 4. In case of hydrolysis by CBH I and CBH II, all soluble sugars except cellobiose, glucose, and cellotriose were produced in negligible amounts (less than 0.01 mg/L, data not reported).

Endo–exo synergism

The endo–exo synergism is a highly effective synergism that has been reported in many studies and plays critical role in the hydrolysis rates and yields (Andersen 2007; Medve et al. 1998; Väljamäe et al. 1999; Zhang and Lynd 2004). The model was simulated for hydrolysis of filter paper and cotton for individual and combined EG and CBH I. Simulations were performed for 48 h assuming 25 g/L substrate concentration at enzyme loadings of 10 mg/g glucans (individually and total of 20 mg/g glucans in mixture, with EG to CBH I ratio of 1:1). Figure 16 illustrates the comparison between theoretical conversion (addition of cellulose conversions during hydrolysis by individual enzymes) and actual conversion (cellulose conversion during hydrolysis by enzymes acting simultaneously).

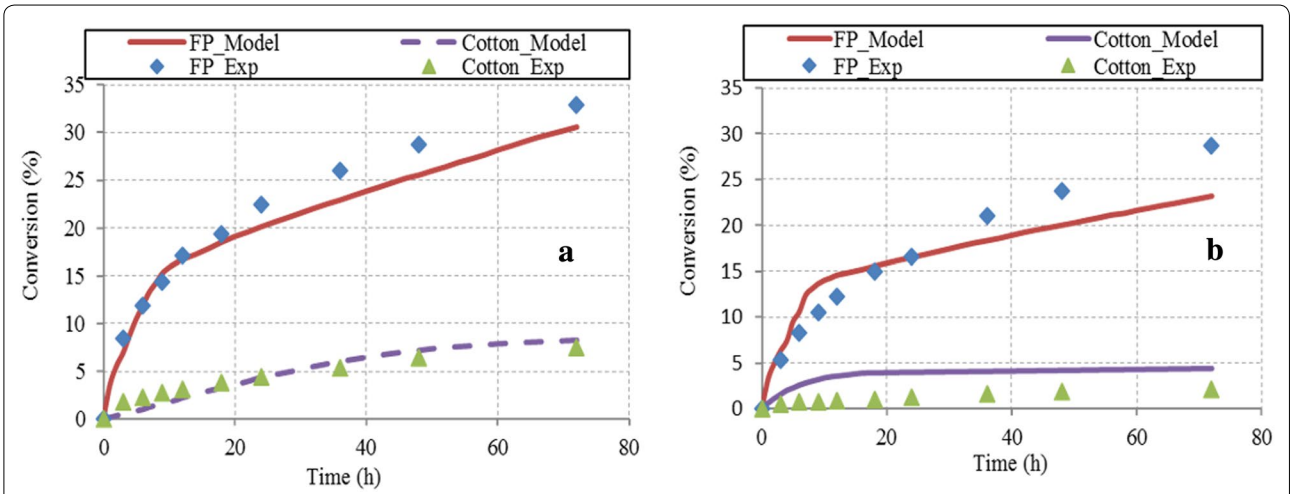

Fig. 14 Effect of cellulose structural properties on hydrolysis: cellulose conversion during hydrolysis of filter paper and cotton (25 g/L) by action of **a** CBH I at loading of 10 mg/g cellulose **b** CBH II at loading of 10 mg/g cellulose

The common measure of synergism is "Degree of synergism (DS)", which is defined as follows (Eq. 2):

$$\text{Degree of synergism} = \frac{\Delta C_{\text{mixed}}}{\sum_{i=1}^{n} \Delta C_i}, \quad (2)$$

where ΔC_{mixed} is cellulose conversion obtained from mixture of 'n' enzymes; ΔC_i is cellulose conversion obtained from an individual action of 'ith' enzyme.

It can be seen from Fig. 16 that the expected synergism was observed in the model simulations. The degree of synergism increased initially and then decreased towards the end of hydrolysis. Similar trends have been observed by other researchers: Kleman-Leyer et al. (1996) for hydrolysis of cotton and Medve et al. (1998) for hydrolysis of Avicel. The phenomenon can be explained by the fact that at the beginning of hydrolysis, the surface molecules are accessible for EG action, and chain ends were sufficient for CBH action. As the hydrolysis progresses, endoglucanases create additional chain ends and increase their availability for exoglucanases, which results in high hydrolysis rate and synergism. However, with further progress in hydrolysis, product (cellobiose and glucose mainly) inhibition becomes very dominant and total yields are not significantly higher than the case where the enzymes work individually. The highest values of degree of synergism were 1.33 and 4.35 for filter paper and cotton, respectively. The values of DS obtained from model simulations are consistent with the reported values in literature (Medve et al. 1998; Väljamäe et al. 1999; Zhang and Lynd 2004; Zhou et al. 2010). A large variation in the DS values can be observed in literature studies, possibly because several factors such as total time of hydrolysis, purity of enzymes, activity of enzymes, and enzyme loadings can affect the synergism. The synergism was observed higher for cotton hydrolysis than that of in case of filter paper hydrolysis. The inverse relationship between DS and substrate DP was expected and has been reported in literature (Andersen 2007; Srisodsuk et al. 1998; Zhang and Lynd 2004). A comprehensive review on hydrolysis from Zhang and Lynd (2004) compiled DS values from various studies and reported low DS values (1.3–2.2) for Avicel and high DS values (4.1–10) for cotton and bacterial cellulose from synergism of *T. reeesi* enzymes. During cellulose hydrolysis by only CBH I, its accessibility to chain ends is very limited and cellulose conversion is very less. The accessibility is further reduced for substrates like cotton, with very high degree of polymerization. During combined action of EG and CBH I, creation of additional chain ends by random action of EG increases the substrate availability for action of CBH I, which results in more effective hydrolysis.

Conclusions

A novel approach of stochastic molecular modeling based on basic sciences and computer algorithms was used to model complex cellulose hydrolysis process. In this work, the model was further improved by incorporating some critical phenomenon, especially the enzyme crowding effect, and the model was validated with actual hydrolysis experiments using purified enzymes. Model was

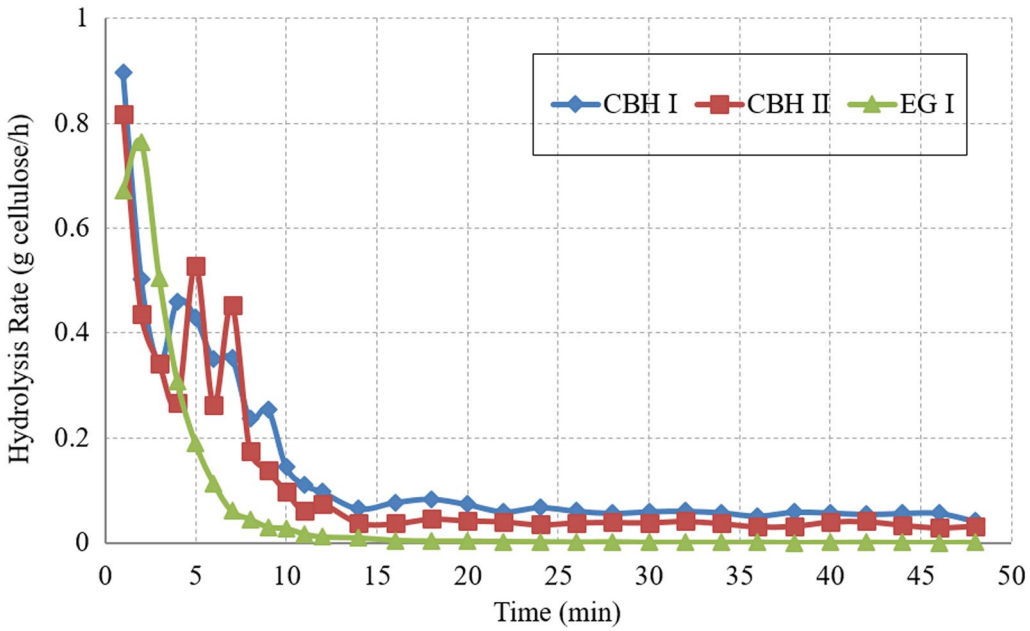

Fig. 15 Model predictions of hydrolysis rate by action of individual enzymes on filter paper (filter paper, 25 g/L; all enzymes, 10 mg/g glucans)

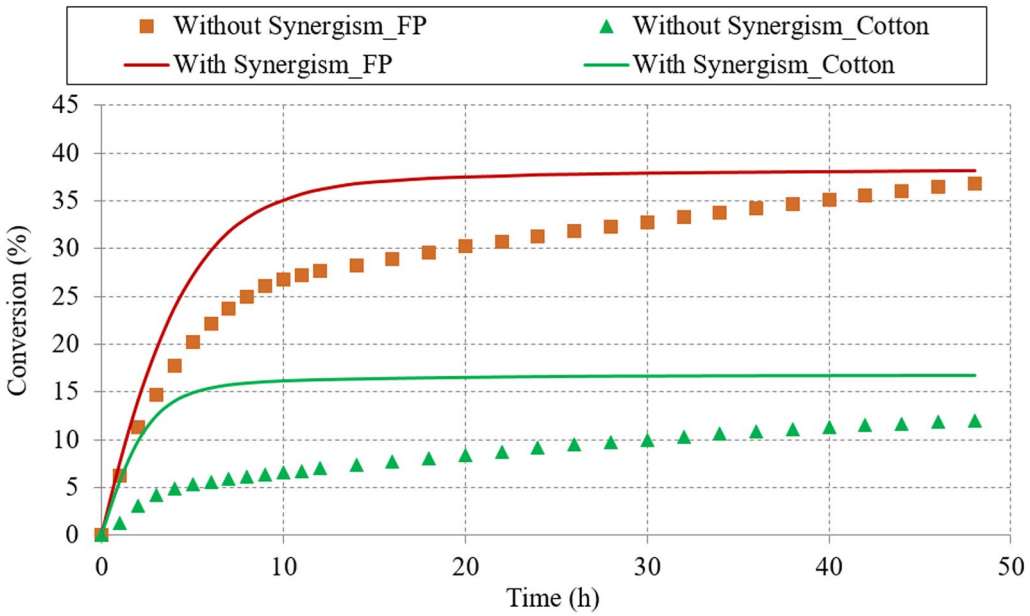

Fig. 16 Endo–exo synergism during hydrolysis of filter paper and cotton cellulose 25 g/L, EG I 10 mg/g glucans, CBHI 10 mg/g glucans (total 20 mg enzymes when acting in mixture 1:1). Solid lines are results from combined action of enzymes and lines with points (theoretical) are sum of conversions from action of individual enzymes

accurate in predicting the cellulose hydrolysis profiles obtained from experimental studies from both literature as well as this work. The model captured the dynamics of cellulose hydrolysis during action of individual as well as multiple cellulase enzymes. Model results successfully followed all important trends, such as product inhibition, low cellobiohydrolase activity on high DP substrates, low endoglucanases activity on crystalline substrate, inverse relationship between degree of synergism and substrate DP, observed experimentally and reported in literature studies. The model was robust and has high potential usability as could be observed from the fact that model simulations fitted well with the experimental data from both literature as well as current work, without changes to any model parameters (except enzyme activity).

Additional files

Additional file 1. Schematic of algorithm for CBH action for cellulose hydrolysis.

Additional file 2. Schematic of algorithm for EG action for cellulose hydrolysis.

Additional file 3: Table S1. Values of parameters used for EG I, CBH I and CBH II action; **Figure S1.** Comparison of model simulations (previous and new version) with experimental data from literature: S1a for Avicel (50 g/L) and S1b for Avicel (25 g/L); **Figure S2.** Comparison of model simulations (old version and current model) with experimental data during hydrolysis of filter paper by CBH I; **Figure S3.** Endoglucanases action on substrates with different crystallinity; **Figure S4.** Glucose production profile during action of endoglucanases on filter paper.

Authors' contributions

DK, and GM developed the model and designed experiments. DK conducted experiments, analyzed data and prepared the manuscript. GM reviewed the results, helped in data analysis and edited the manuscript. All authors read and approved the final manuscript.

Author details

[1] Biological and Ecological Engineering, Oregon State University, Corvallis, OR, USA. [2] Agricultural and Biological Engineering, University of Illinois at Urbana-Champaign, Urbana, IL, USA.

Acknowledgements

Authors gratefully acknowledge the support by National Science Foundation through NSF Grant No. 1236349 from Energy for Sustainability program, CBET Division.

Competing interests

The authors declare that they have no competing interests.

Availability of data and materials

All data generated and analyzed during this study are included in within the manuscript in the form of graphs and tables. The authors promise to provide any missing data on request.

Consent for publication

Not applicable.

Ethical approval and consent to participate

Not applicable.

Publisher's Note

Received: 20 September 2017 Accepted: 30 November 2017
Published online: 12 December 2017

References

Andersen N (2007) Enzymatic hydrolysis of cellulose—experimental and modeling studies. Technical University of Denmark, Copenhagen

Andersen N, Johansen KS, Michelsen M, Stenby EH, Krogh KBRM, Olsson L (2008) Hydrolysis of cellulose using mono-component enzymes shows synergy during hydrolysis of phosphoric acid swollen cellulose (PASC), but competition on Avicel. Enzym Microb Technol 42:362–370

Asztalos A, Daniels M, Sethi A, Shen T, Langan P, Redondo A, Gnanakaran S (2012) A coarse-grained model for synergistic action of multiple enzymes on cellulose. Biotechnol Biofuels 5:55

Baker JO, Ehrman CI, Adney WS, Thomas SR, Himmel ME (1998) Hydrolysis of cellulose using ternary mixtures of purified celluloses. Appl Biochem Biotechnol 70:395–403

Ballesteros M (2010) Enzymatic hydrolysis of lignocellulosic biomass. In: Waldron K (ed) Bioalcohol production: biochemical conversion of lignocellulosic biomass. CRC Press, Boca Raton

Banerjee G, Car S, Scott-Craig JS, Borrusch MS, Bongers M, Walton JD (2010a) Synthetic multi-component enzyme mixtures for deconstruction of lignocellulosic biomass. Bioresour Technol 101:9097–9105

Banerjee G, Car S, Scott-Craig JS, Borrusch MS, Walton JD (2010b) Rapid optimization of enzyme mixtures for deconstruction of diverse pretreatment/biomass feedstock combinations. Biotechnol Biofuels 3:22

Bansal P, Hall M, Realff MJ, Lee JH, Bommarius AS (2009) Modeling cellulase kinetics on lignocellulosic substrates. Biotechnol Adv 27:833–848

Berlin A, Maximenko V, Gilkes N, Saddler J (2007) Optimization of enzyme complexes for lignocellulose hydrolysis. Biotechnol Bioeng 97:287–296

Besselink T, Baks T, Janssen AEM, Boom RM (2008) A stochastic model for predicting dextrose equivalent and saccharide composition during hydrolysis of starch by α-amylase. Biotechnol Bioeng 100:684–697

Bezerra RMF, Dias AA (2004) Discrimination among eight modified Michaelis-Menten kinetics models of cellulose hydrolysis with a large range of substrate/enzyme ratios. Appl Biochem Biotechnol 112:173–184

Bezerra RMF, Dias AA, Fraga I, Pereira AN (2011) Cellulose hydrolysis by cellobiohydrolase Cel7A Shows mixed hyperbolic product inhibition. Appl Biochem Biotechnol 165:178–189

Chang VS, Holtzapple MT (2000) Fundamental factors affecting biomass enzymatic reactivity. Appl Biochem Biotechnol 84:5–37

Chinga-Carrasco G (2011) Cellulose fibres, nanofibrils and microfibrils: the morphological sequence of MFC components from a plant physiology and fibre technology point of view. Nanoscale Res Lett 6:417

Eriksson T, Karlsson J, Tjerneld F (2002) A model explaining declining rate in hydrolysis of lignocellulose substrates with cellobiohydrolase I (Cel7A) and endoglucanase I (Cel7B) of *Trichoderma reesei*. Appl Biochem Biotechnol 101:41–60

Fan L, Lee Y (1983) Kinetic studies of enzymatic hydrolysis of insoluble cellulose: derivation of a mechanistic kinetic model. Biotechnol Bioeng 25:2707–2733

Fan L, Gharpuray MM, Lee YH (1987) Cellulose hydrolysis. Biotechnology monographs, vol 3. Springer, Berlin

Gao D, Chundawat SPS, Krishnan C, Balan V, Dale BE (2010) Mixture optimization of six core glycosyl hydrolases for maximizing saccharification of ammonia fiber expansion (AFEX) pretreated corn stover. Bioresour Technol 101:2770–2781

Ghose T (1987) Measurement of cellulase activities. Pure Appl Chem 59:257–268

Hall M, Bansal P, Lee JH, Realff MJ, Bommarius AS (2010) Cellulose crystallinity—a key predictor of the enzymatic hydrolysis rate. FEBS J 277:1571–1582

Igarashi K et al (2011) Traffic jams reduce hydrolytic efficiency of cellulase on cellulose surface. Science 333:1279–1282

Jäger G et al (2010) Practical screening of purified cellobiohydrolases and endoglucanases with α-cellulose and specification of hydrodynamics. Biotechnol Biofuels 3:18

Jeoh T, Ishizawa CI, Davis MF, Himmel ME, Adney WS, Johnson DK (2007) Cellulase digestibility of pretreated biomass is limited by cellulose accessibility. Biotechnol Bioeng 98:112–122

Kadam KL, Rydholm EC, McMillan JD (2004) Development and validation of a kinetic model for enzymatic saccharification of lignocellulosic biomass. Biotechnol Prog 20:698–705

Kleman-Leyer KM, Siika-Aho M, Teeri TT, Kirk TK (1996) The cellulases endoglucanase I and cellobiohydrolase II of Trichoderma reesei act synergistically to solubilize native cotton cellulose but not to decrease Its molecular size. Appl Environ Microbiol 62:2883–2887

Kumar D (2014) Biochemical conversion of lignocellulosic biomass to ethanol: experimental, enzymatic hydrolysis modeling, techno-economic and life cycle assessment studies. Oregon State University, Corvallis

Kumar D, Murthy GS (2011) Impact of pretreatment and downstream processing technologies on economics and energy in cellulosic ethanol production. Biotechnol Biofuels 4:27

Kumar D, Murthy GS (2013) Stochastic molecular model of enzymatic hydrolysis of cellulose for ethanol production. Biotechnol Biofuels 6:63

Levine SE, Fox JM, Blanch HW, Clark DS (2010) A mechanistic model of the enzymatic hydrolysis of cellulose. Biotechnol Bioeng 107:37–51

Lynd LR, Weimer PJ, Van Zyl WH, Pretorius IS (2002) Microbial cellulose utilization: fundamentals and biotechnology. Microbiol Mol Biol Rev 66:506–577

Marchal L, Zondervan J, Bergsma J, Beeftink H, Tramper J (2001) Monte Carlo simulation of the α-amylolysis of amylopectin potato starch. Bioprocess Biosyst Eng 24:163–170

Marchal L, Ulijn R, Gooijer CD, Franke G, Tramper J (2003) Monte Carlo simulation of the α-amylolysis of amylopectin potato starch. 2. α-amylolysis of amylopectin. Bioprocess Biosyst Eng 26:123–132

Matsumoto M, Nishimura T (1998) Mersenne twister: a 623-dimensionally equidistributed uniform pseudo-random number generator. ACM Trans Model Comput Simul 8:3–30

Medve J, Karlsson J, Lee D, Tjerneld F (1998) Hydrolysis of microcrystalline cellulose by cellobiohydrolase I and endoglucanase II from *Trichoderma reesei*: adsorption, sugar production pattern, and synergism of the enzymes. Biotechnol Bioeng 59:621–634

Merino S, Cherry J (2007) Progress and challenges in enzyme development for biomass utilization. Biofuels 108:95–120

Mosier N, Hall P, Ladisch C, Ladisch M (1999) Reaction kinetics, molecular action, and mechanisms of cellulolytic proteins. Recent Progress Bioconversion Lignocellul 65:23–40

Murthy GS, Johnston DB, Rausch KD, Tumbleson M, Singh V (2011) Starch hydrolysis modeling: application to fuel ethanol production. Bioprocess Biosyst Eng 34:879–890

Sangseethong K, Penner MH (1998) *p*-Aminophenyl β-cellobioside as an affinity ligand for exo-type cellulases. Carbohydr Res 314:245–250

Srisodsuk M, Kleman-Leyer K, Keränen S, Kirk TK, Teeri TT (1998) Modes of action on cotton and bacterial cellulose of a homologous endoglucanase–exoglucanase pair from *Trichoderma reesei*. Eur J Biochem 251:885–892

Teugjas H, Väljamäe P (2013) Product inhibition of cellulases studied with ^{14}C-labeled cellulose substrates. Biotechnol Biofuels 6:104

Väljamäe P, Sild V, Nutt A, Pettersson G, Johansson G (1999) Acid hydrolysis of bacterial cellulose reveals different modes of synergistic action between cellobiohydrolase I and endoglucanase I. Eur J Biochem 266:327–334

Wang M, Li Z, Fang X, Wang L, Qu Y (2012) Cellulolytic enzyme production and enzymatic hydrolysis for second-generation bioethanol production. Adv Biochem Eng Biotechnol. 128:1–24. https://doi.org/10.1007/10_2011_131

Wojciechowski PM, Koziol A, Noworyta A (2001) Iteration model of starch hydrolysis by amylolytic enzymes. Biotechnol Bioeng 75:530–539

Wood T (1974) Properties and mode of action of cellulases. In: Biotechnology and bioengineering symposium, vol 5, pp 111–133

Zhang YHP, Lynd LR (2004) Toward an aggregated understanding of enzymatic hydrolysis of cellulose: noncomplexed cellulase systems. Biotechnol Bioeng 88:797–824

Zhang YHP, Lynd LR (2006) A functionally based model for hydrolysis of cellulose by fungal cellulase. Biotechnol Bioeng 94:888–898

Zhou W, Hao Z, Xu Y, Schüttler HB (2009) Cellulose hydrolysis in evolving substrate morphologies II: numerical results and analysis. Biotechnol Bioeng 104:275–289

Zhou W, Xu Y, Schüttler HB (2010) Cellulose hydrolysis in evolving substrate morphologies III: time-scale analysis. Biotechnol Bioeng 107:224–234